Compact Lowpass Filter with Wide Stop-Band using Open Stubs-Loaded Spiral Microstrip Resonant Cell

Auob Adinehvand and Ali Lotfi

Computer Engineering Department, Faculty of Engineering, Islamic Azad University,
Kermanshah Branch, Kermanshah, Iran
auobadinehvand@yahoo.com and lotfi_electrical@yahoo.com

Abstract ─ In this paper, a compact lowpass filter using open stubs-loaded spiral compact microstrip resonant cell (OSL-SCMRC) is presented. The proposed resonator is implemented to design the lowpass filter with the wide and high out-of-band rejection in the stop-band region. The lowpass filter has the insertion loss from DC to 5.29 GHz better than -0.1 dB and the return loss better than -19.3 dB. Moreover, the lowpass filter is shown to suppress the harmonics with -20 dB attenuation level from 6.71 GHz to 16.73 GHz result in a 10.02 GHz rejection band. The proposed resonator has an improved slow-wave factor, low radiation and scattering, with a compact size. The filter is designed, fabricated and measured. There is a good agreement between the measured and the simulated S-parameters.

Index Terms ─ Low insertion loss, lowpass filter, microstrip resonator cell, open stubs-loaded, and wide stop-band.

I. INTRODUCTION

Microstrip lowpass filter (LPF) with low insertion loss and broad stop-band are in high demand for the microwave communication systems. To meet the size requirement of the modern microwave circuits, several techniques have been proposed. One of the most interesting and popular techniques is planar resonators. These resonators due to their compact size and easy fabrication have been taken into consideration for the microwave filter design increasingly. Moreover, this resonator has a shortcoming such as: high insertion loss in the pass-band, restricted stop-band, and return loss that limits the engineering applications of these resonators, hence several methods are employed to overcome these drawbacks.

One of the interested with high demanded techniques for the syntheses of the microstrip LPF is the structure that use the photonic band gap (PBG). The one-dimension (1-D) compact microstrip resonant cell (CMRC) was presented in [1]. The use of one-dimensional (1-D) photonic band gap cell exhibits remarkable slow-wave and bandstop performance with quasi–lumped circuit element. Spiral compact microstrip resonant cell (SCMRC) and compensated spiral compact microstrip resonant cells (C-SCMRC) are proposed in [2] and [3], respectively. It has been shown that the resonator can further enhance the slow-wave effect for the circuit size reduction and enlarge the stop-band bandwidth for better performance, and it can achieve the goal of the deep suppression of harmonics. The rectangular patch CMRC (RPCMRC) and defected ground structure are proposed in [4], while the CMRC based on the defected ground structure is proposed in [5]. However, these two structures owing to etching in the ground plane cannot have application on the metal surface and cannot give a robust mechanical endurance against the strain. A tapered periodical CMRC topology with non-uniform cell dimension is proposed to develop a lowpass filter [6].

The lowpass filter using a SCMRC proposed in [7] suffers from two drawbacks, i.e., high insertion loss in the pass-band and a restricted stop-band. Other types of the CMRC configurations have been proposed such as: a slit-loaded tapered CMRC (SL-TCMRC) in order to develop a lowpass filter [8], a front coupled

Submitted On: Sep. 11, 2012
Accepted On: Dec. 21, 2012

tapered CMRC (FC-TCMRC) [9], and a comb compact microstrip resonant cell (CCMRC) [10]. Other techniques have been proposed for the syntheses of the microstrip lowpass filter such as: the miniaturized stepped impedance [11], open loop resonators [12], triangular patch resonator with fractal defection [13], the meander open-loop resonator for syntheses of lowpass filter [14], and photonic band-gap structure (PBG) [15-20]. Although, all these structures have low insertion loss and compact size, the wide stop-band with its superior suppression remain the main challenge for the proposed filters. The open stub-loaded spiral compact microstrip resonant cell (OSL-SCMRC) is proposed in order to design a lowpass filter with low insertion loss in the pass-band, with a wide stop-band and compact size.

The proposed structure is simulated using an EM-simulator (ADS), fabricated and measured. The simulation and measurement results show enhanced performance of the designed filter in the pass-band and stop-band regions. Both results are illustrated, and good agreement between them is achieved.

II. DESIGN OF THE FILTER STRUCTURE

Figure1 shows our designed, open stubs-loaded spiral compact microstrip resonant cell (OSL-SCMRC). The inductance and capacitance obtained from CMRC will be enhanced without any additional lumped components. Due to the added transmission zeros in the stop-band, the new resonator has extended stop-band and improved slow-wave characteristics, which leads to circuit size reduction.

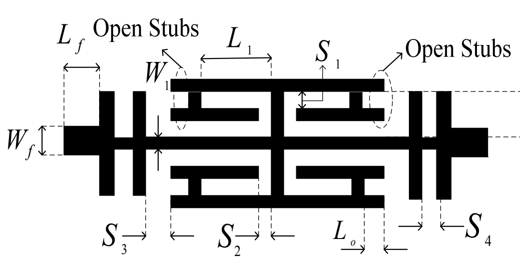

Fig. 1. Schematic diagram of the proposed OSL-SCMRC.

The transmission-line model of the proposed open stubs-loaded spiral compact microstrip resonant cell (OSL-SCMRC) is shown in Fig. 2.

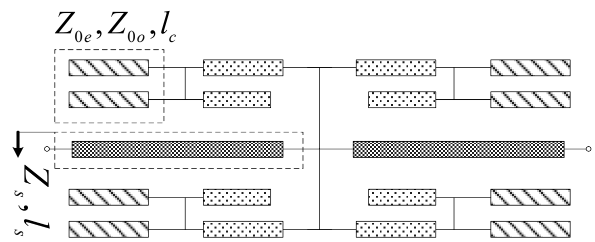

Fig. 2. Transmission line model of the proposed OSL-SCMRC.

It can be noticed from Fig. 2 that the model is composed of two-coupled transmission lines and a central narrow micorstrip line. The equivalent circuit of the two coupled transmission lines and a single transmission line model are shown in Fig. 3 (a) and (b), respectively.

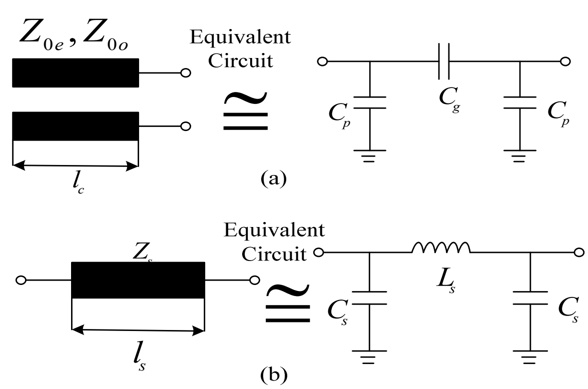

Fig. 3. (a) Two-coupled transmission line model with its equivalent circuit, (b) Single transmission line model with its equivalent circuit.

The symmetric parallel coupled lines are modelled as an equivalent capacitive π-network and the *ABCD* matrix of the lossless parallel coupled lines is expressed as [21],

$$\begin{bmatrix} A_1 & B_1 \\ C_1 & D_1 \end{bmatrix} = \begin{bmatrix} \dfrac{Z_{0e}+Z_{0o}}{Z_{0e}-Z_{0o}} & \dfrac{-j2Z_{0e}Z_{0o}\cot(\beta_c l_c)}{Z_{0e}-Z_{0o}} \\ \dfrac{-j2}{(Z_{0e}-Z_{0o})\cot(\beta_c l_c)} & \dfrac{Z_{0e}+Z_{0o}}{Z_{0e}-Z_{0o}} \end{bmatrix} \quad (1)$$

where β_c is the phase constant of the coupled lines. The *ABCD* matrix of the equivalent capacitive π - network can be obtained as follow,

$$\begin{bmatrix} A_1 & B_1 \\ C_1 & D_1 \end{bmatrix} = \begin{bmatrix} 1+Z_g Y_p & Z_g \\ Y_p(2+Z_g Y_p) & 1+Z_g Y_p \end{bmatrix}. \tag{2}$$

In equation (2), $Z_g = 1/j\omega C_g$ and $Y_p = j\omega C_p$. From equations (1) and (2), the equivalent capacitances of the π -network can be written as,

$$C_g = \frac{Z_{0e} - Z_{0o}}{2\omega Z_{0e} Z_{0o} \cot(\beta_c l_c)}.(F) \tag{3-a}$$

$$C_p = \frac{1}{\omega Z_{0e} \cot(\beta_c l_c)}.(F)\cdot \tag{3-b}$$

The single transmission line is shown in Fig. 3 (b), this transmission line can be modelled as an equivalent *L-C* π -network. The *ABCD* matrix can be defined as,

$$\begin{bmatrix} A_2 & B_2 \\ C_2 & D_2 \end{bmatrix} = \begin{bmatrix} \cos(\beta_s l_s) & jZ_s \sin(\beta_s l_s) \\ jY_s \sin(\beta_s l_s) & \cos(\beta_s l_s) \end{bmatrix}. \tag{4}$$

In equation (4) the phase constant and the characteristic admittance of the single transmission line can be defined as β_s and $Y_s = 1/Z_s$, respectively. The *ABCD* matrix of the equivalent *L-C* π -network is defined as,

$$\begin{bmatrix} A_2 & B_2 \\ C_2 & D_2 \end{bmatrix} = \begin{bmatrix} 1+Z_L Y_c & Z_L \\ Y_c(2+Z_L Y_c) & 1+Z_L Y_c \end{bmatrix} \tag{5}$$

where $Z_L = j\omega L_s$ and $Y_c = j\omega C_s$, in which L_s and C_s are the equivalent inductance and capacitance of the single transmission line. The angular frequency is defined as ω, from equations (4) and (5) the value of L_s and C_s are expressed by,

$$L_s = \frac{Z_s \sin(\beta_s l_s)}{\omega}.(H) \tag{6-a}$$

$$C_s = \frac{1-\cos(\beta_s l_s)}{\omega Z_s \sin(\beta_s l_s)}.(F)\ \cdot \tag{6-b}$$

Therefore, the *ABCD* matrix of the proposed resonator can be used to describe the electrical characteristics and performance predication of the open stubs-loaded spiral compact microstrip resonant cell (OSL-SCMRC). It can be clearly observed that increasing the capacitance within the structure is by using a gap between the central narrow line and open stubs, so it can give attenuation poles in the stop-band. Consequently, it will have a wide stop-band. The demonstrated resonator is implemented on (RT/Duroid 5880) substrate with relative permittivity equals to 2.2, thickness of 10 mil, and a loss tangent equals to 0.0009. The simulated S-parameters of the proposed resonator as functions of L_1, L_o and S_1 are shown in Fig. 4 (a), (b), and (c), respectively.

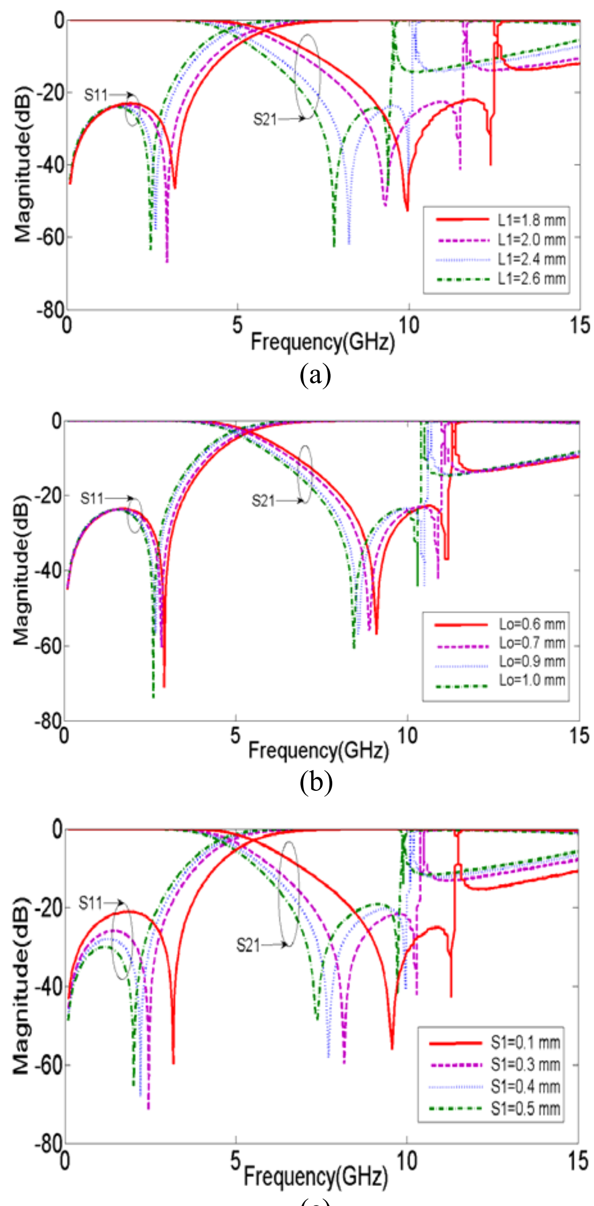

Fig. 4. (a) S-parameters simulation of the proposed resonator as a function of L_1, (b) S-parameters simulation of the proposed resonator as a function of L_o, and (c) S-parameters simulation of the proposed resonator as a function of S_1.

As seen in Fig. 4 (a), when L_1 increases from 1.8 mm to 2.6 mm, the transmission zero at 9.96 GHz approaches the lower frequency. Similarly, in Fig. 4 (b) by decreasing L_o from 1.0 mm to 0.6 mm, the transmission zero at 8.44 GHz starts to move away from the lower frequency. In Fig. 4 (c) by decreasing S_1 from 0.5 mm to 0.1 mm due to the decrement of the effective series inductance, the transmission zero at 7.39 GHz also starts to move away from the lower frequency. Hence, the location of transmission zeros can be controlled by a parallel capacitance with a series inductance, as the attenuation zeros location became lower, which is due to the increment of the series inductance and the decrement of the resonant frequency of the equivalent LC circuit. This can be concluded from Fig. 2 and the equivalent circuit elements defined in equation (1) to equation (6).

The two neighbouring open stubs are coupled, which not only enhance the equivalent capacitance of the loading capacitor, but also provide the finite attenuation poles. If the dimensions of the internal open stubs are arbitrarily selected, the harmonics and the spurious will not be suppressed well, and only a narrow rejection bandwidth will be obtained.

Therefore, the internal open stubs need to be optimized. The dimensions of the proposed structure shown in Fig. 1 are as follows: L_1 = 2.2, L_2 = 0.8, L_o = 0.8, S_1 = 0.2, S_2 = 0.2, S_3 = 0.2, S_4 = 0.2, W_1 = 0.2, L_f = 0.7, and W_f = 0.6 (all in mm). The simulated S-parameters of the proposed resonator with these dimensions are shown in Fig. 5, the stop-band has been observed from 7.75 GHz to 10.80 GHz, with -20 dB, and from 6.55 GHz to 10.85 GHz with -10dB attenuation level. The insertion loss from DC to 4.45 GHz is less than -1 dB, and the return loss in the pass-band is better than -28 dB. The return loss in the stop-band is close to 0 dB. Therefore, the small radiation loss can be ignored. The radiation and the scattering effects of the open stubs-loaded spiral compact microstrip resonant cell (OSL-SCMRC) are defined by $1-|S_{11}|^2-|S_{21}|^2$ and are shown in Fig. 6 (a). The radiation and the scattering effects are maintained at low levels while the operating frequency is below 10.9 GHz. The maximum percentage of both, radiation and scattering is 39.44%.

The slow-wave factor (SWF) of the open stubs-loaded spiral compact microstrip resonant cell is defined as follows,

$$SWF = \frac{\lambda_0 \Delta\theta}{360L} + \sqrt{\varepsilon_{eff}} \tag{7}$$

$$\varepsilon_{eff} = \frac{\varepsilon_r + 1}{2} + \frac{\varepsilon_r - 1}{2}\left(1 + 12\frac{h}{W}\right)^{-0.5}, \tag{8}$$

where L and W are the length and width of the microstrip line, respectively. The symbol λ_0 is the free space wavelength, $\Delta\theta$ is the phase difference (in degrees) between the conventional microstrip and the OSL-SCMRC. Finally, ε_{eff} is the effective microstrip permittivity.

Figure 6 (b) shows a comparison between the slow-wave factor (SWF) of the conventional microstrip line and the OSL-SCMRC. It can be seen that the obtained SWF of the conventional microstrip line is 1.357 in the pass-band region at 5.3 GHz, where the proposed OSL-SCMRC increased the SWF by 335.88% to 5.915.

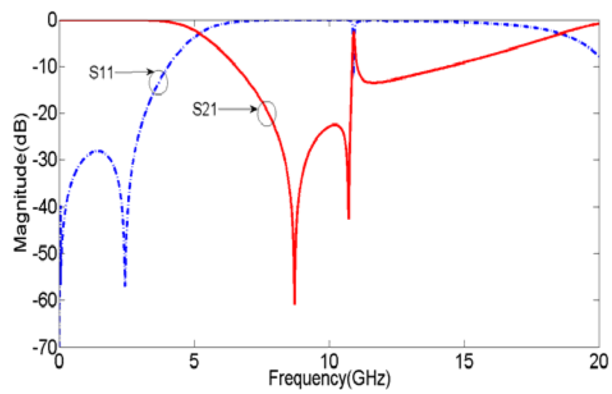

Fig. 5. S-parameter simulation of the proposed resonator.

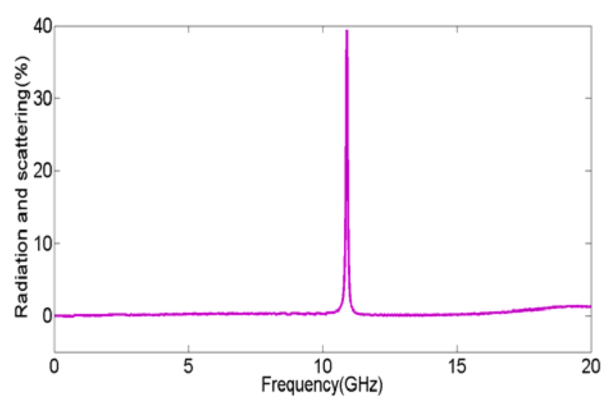

(a)

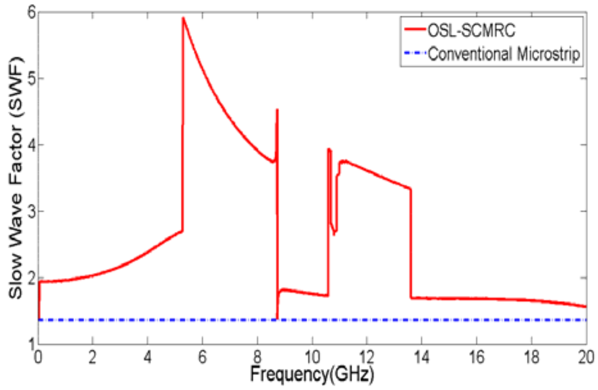

(b)

Fig. 6. (a) Radiation and scattering effects of the proposed OSL-SCMRC and (b) slow-wave factor of the proposed OSL-SCMRC and the conventional microstrip.

The results reveal that the SWF of the conventional microstrip line is improved by using OSL-SCMRC. So the size of the proposed lowpass filter has been reduced as compared to the lowpass filter using the conventional SCMRC. Furthermore, the effect of the coupled capacitance can suppress the first spurious stop-band response near the pass-band, so the actual stop-band of such lowpass filter can be extended.

By connecting several resonators in series form, the periodic structure presents manifest slow-wave effect and bandstop characteristics. The resonators with periodic structures and different dimensions, because of their different cutoff frequency, results in obtaining the lowpass filter with wide stop-band; hence the flaw in stop-band was avoided.

III. SIMULATION AND MEASUREMENT RESULTS

The lowpass filter in the stop-band region exhibits harmonics, thus the stop-band is restricted. To overcome this problem, three resonators with different dimensions cascaded in a series form are designed and their dimensions were optimized to gain a wide stop-band with a compact size. The wide stop-band can be achieved because of the resonators with the multi cutoff frequencies.

The EM–simulator (ADS) is used for the optimization of the dimensions of the resonator to obtain the LPF as shown in Fig. 7, with the desired characteristics.

As shown in Fig. 8 (a) by increasing S_1 from 0.1 mm to 0.4 mm, the S_{21} is attenuated. Therefore, the suppression of the unwanted harmonic in the stop-band can be achieved. In Fig. 8 (b) L_1 has increased from 1.8 mm to 2.6 mm, and the transmission zero at 9.84 GHz has been moved to a lower frequency. Consequently, the transmission zeros in the stop-band can be easily controlled by the dimensions of the proposed resonator. The dimensions of the obtained LPF shown in Fig. 7 are: L_1 = 2.2, S_3 = 0.2, S_1 = 0.2, L_o = 0.8, L_{21} = 1.5, L_{22} = 0.5, L_{2o} = 0.4, S_{21} = 0.1, S_{22} = 0.2, S_{23} = 0.3, S_{24} = 0.1, W_{22} = 0.4, L_s = 0.3, L_f = 1, and W_f = 0.6 (all in mm).

The photograph of the fabricated filter is shown in Fig. 9 (a). The filter has a size of 20 mm × 1.8 mm. The design is verified by an EM-simulator (ADS), and the measurement is done using an Agilent Network Analyzer N5230A. Both simulation and measurement results of the lowpass filter using OSL-SCMRC structure are illustrated in Fig. 9 (b). Obviously, the lowpass filter behaves well in the pass-band and stop-band regions. As seen from Fig. 9 (b), the designed filter has an insertion loss from DC to 5.29 GHz better than -0.1 dB and a return loss better than -19.3 dB and even reaches to -41.5 dB at 2.25 GHz, where the transmission pole is located.

The stop-band region, from 6.71 GHz to 16.73 GHz with -20 dB attenuation level, result in a 10.02 GHz rejection band. This is considered a wide rejection band. The designed filter has two transmission zeros, 7.11 GHz with -56.13 dB and 7.91 GHz with -68.09 dB. This results in a sharp skirt characteristic to the lowpass filter. Obviously, the two symmetrical open stubs-loaded spiral compact microstrip resonant cells (OSL-SCMRC) patches can help to achieve a wide stop-band. Hence our design has low insertion loss, wide stop-band, and a very compact size. The proposed resonator can be easily tuned to the desired frequency by adjusting the length of the open stubs. Therefore, it can be employed in the microwave applications.

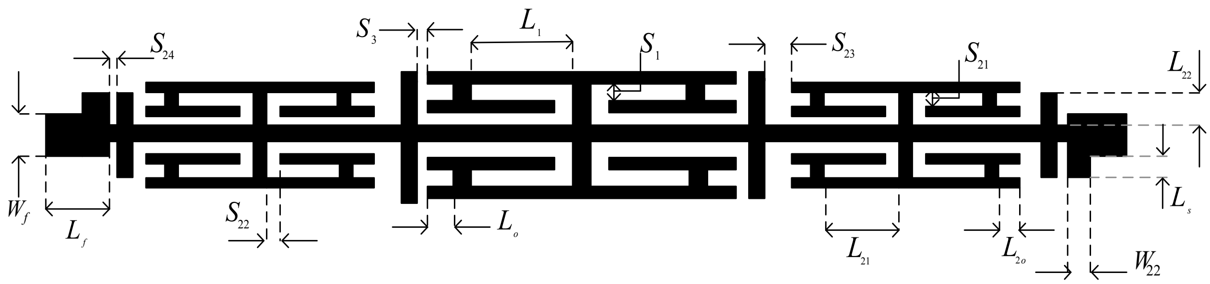

Fig. 7. Schematic diagram of the designed LPF.

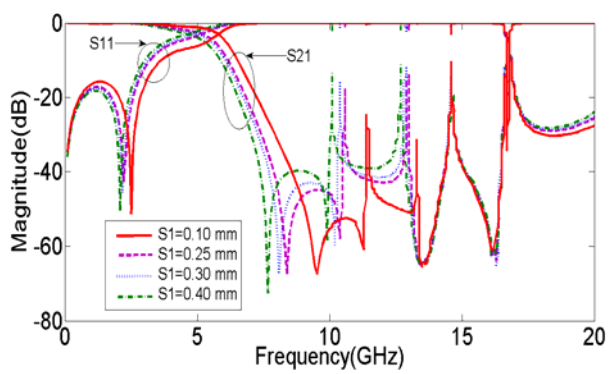

(a)

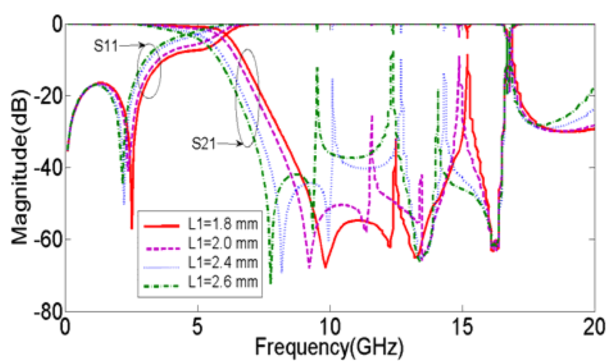

(b)

Fig. 8. Simulated S-parameters of the designed LPF as a function of (a) S_1 and (b) L_1.

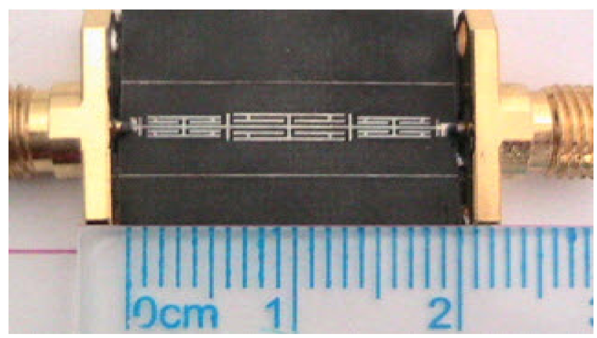

(a)

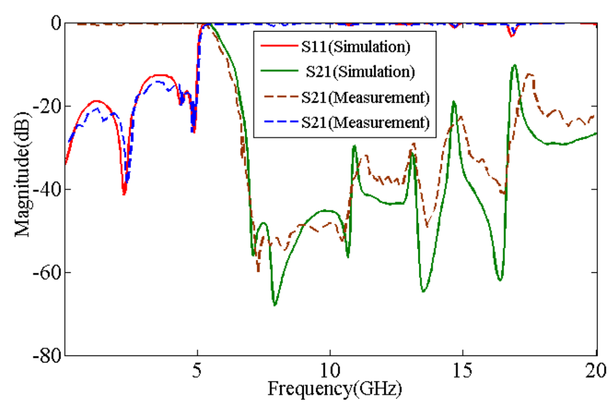

(b)

Fig. 9. (a) The photograph of the fabricated filter and (b) the simulated and measured S-parameters of the proposed LPF.

IV. CONCLUSION

In this work, a novel compact microstrip lowpass filter using an open stubs-loaded spiral compact microstrip resonant cell is presented. The proposed structure of the lowpass filter has some good characteristics. The designed resonator has low radiation and scattering effects due to the lower relative permittivity constant and thinned out substrate. The lowpass filter has low insertion loss in the pass-band region, high return loss, wide stop-band region, and a very compact size. The designed filter uses resonators of different dimensions with different cutoff frequencies, resulting in a wide stop-band. The measured and simulated results are in good agreement. The designed structure can be employed, where lowpass filters with the wide stop-band, high return loss, low insertion loss, and compact size are needed in the microwave applications.

REFERENCES

[1] Q. Xue, K. M. Shum, and C. H. Chan, "Novel 1-D microstrip PBG cells," *IEEE Microwave and Guided Wave Letters*, vol. 10, no. 10, pp. 403-405, Oct. 2000.

[2] T. Y. Yum, Q. Xue, and C. H. Chan, "Novel sub harmonically pumped mixer incorporating dual-band stub and in-line SCMRC," *IEEE Trans. on Microwave Theory and Technique*, vol. 51, no. 12, pp. 2538-2547, Dec. 2003.

[3] J. Gu and X. Sun, "Miniaturization and harmonic suppression rat-race coupler using C-SCMRC resonators with distributive equivalent circuit structure," *IEEE Microwave and Wireless Components Letters*, vol. 15, no. 12, pp. 880-882, Dec. 2005.

[4] S. Dwari and S. Sanyal , "Compact wide stop-band lowpass filter using rectangular patch compact microstrip resonant cell and defected ground structure," *Microwave Optical Technology Letters*, vol. 49, no. 4, pp.798-800, April 2007.

[5] Y. -J. Chen, "Novel compact lowpass filter with CMRC based on defected ground structure," *Microwave Optical Technology Letters*, vol. 48, no. 4, pp.695-697, April 2006.

[6] L. Li, Z. F. Li, and Q. F. Wei, "Compact and selective lowpass filter with very wide stop-band using tapered compact microstrip resonant cells," *Electronic Letters*, vol. 45, no. 5, pp. 267-268, Feb. 2009.

[7] J. Gu and X. Sun, "Compact lowpass filter using spiral compact microstrip resonant cells," *Electronic Letters*, vol. 41, no. 19, pp. 1065-1066, Sep. 2005.

[8] M. Hayati and A. Lotfi, "Elliptic-function lowpass filter with sharp cutoff frequency using slit-loaded tapered compact microstrip resonator cell," *Electronic Letters*, vol. 46, no. 2, pp. 143-144, Jan. 2010.

[9] M. Hayati and A. Lotfi, "Compact lowpass filter with high and wide rejection in stop-band using front coupled tapered CMRC," *Electronic Letters*, vol. 46, no. 12, pp. 846-848, June 2010.

[10] C. F. Zhang, "Compact and wide stop-band lowpass filter with novel comb CMRC," *International Journal of Electronics*, vol. 96, no. 7, pp. 749-754, July 2009.

[11] S. -H. Fu, C. -M. Tong, X. -M. Li, W. Zhang, and K. Shen, "Compact miniaturized stepped impedance low-pass filter with sharp cutoff characteristic," *Microwave Optical Technology Letters*, vol. 51, no. 10, pp. 2257-2258, Oct. 2009.

[12] K. R. Jha and N. Nehra, "Microstrip low-pass filter using open loop resonators," *Microwave Optical Technology Letters*, vol. 50, no. 11, pp. 2983-2986, Nov. 2008.

[13] J. -K. Xiao, Q. -X. Chu, and H. -F. Huang, "New microstrip low pass filter with transmission zero and wide stop-band," *Microwave Optical Technology Letters*, vol. 51, no. 3, pp. 830-831, March 2009.

[14] J. X. Chen and Q. Xue, "A novel compact microstrip lowpass filter using a meander open-loop resonator," *Microwave Optical Technology Letters,* vol. 45, no. 1, pp. 66-67, April 2005.

[15] S. K. Parui and S. Das, "A microstrip filter using split-ring PBG to get wide, deep and sharp stop-band," *International Journal of Electronics*, vol. 94, no. 6, pp. 645-652, June 2007.

[16] M. Al Sharkawy, A. Boutejdar, F. Alhefnawi, and O. Luxor, "Improvement of compactness of lowpass/Bandpass filter using a new electromagnetic coupled crescent defected ground structure (DGS) resonators," *Appl. Comp. Electro. Society (ACES) Journal*, vol. 25, no. 9, July 2010.

[17] R. N. Baral and P. K. Singhal, "Design and analysis of micorstrip photonic band gap filter for suppression of periodicity," *Appl. Comp. Electro. Society (ACES) Journal*, vol. 25, no. 2, Feb. 2010.

[18] A. Boutejdar, M. Challal, and A. Azrar , " A novel band-stop filter using octagonal-shaped patterned ground structures along with interdigital and compensated capacitors ," *Appl. Comp. Electro. Society (ACES) Journal*, vol. 26, no. 4, pp. 312-318, April 2011.

[19] F. Karshenas, A. R. Mallahzadeh, and J. Rashed-Mohassel, "Size reduction and harmonic suppression of parallel coupled-line bandpass filters using defected ground structure," *Appl.*

Comp. Electro. Society (ACES) Journal, vol. 25, no. 2, pp. 149-155, Feb. 2010.

[20] N. M. Garmjani and N. Komjani, "Improved microstrip folded tri-section stepped impedance resonator bandpass filter using defected ground structure," *Appl. Comp. Electro. Society (ACES) Journal*, vol. 25, no. 11, pp. 975-983, Nov. 2010.

[21] M. Sagawa, K. Takahashi, and M. Makimot, "Miniaturized hairpin resonator filters and their application to receiver front-end MIC's," *IEEE Trans. on Microwave Theory and Technique*, vol. 37, no. 12, pp. 1991-1997, Dec. 1989.

Auob Adinehvand was born in kouhdasht, Iran in 1982. He received his B.Sc. in Computer Hardware from Islamic Azad University, Arak, Iran in 2007 and M.Sc. in Computer Systems Architecture from the same university in 2009. He is currently working toward the Ph.D. degree in the Department of Electrical Engineering, RAZI University, Kermanshah, Iran. His research interests include QCA circuit design and Microwave active and passive components.

Ali Lotfi received the B.Sc. degree in Electrical Engineering from the Iran University of Science and Technology (I.U.S.T), Tehran, Iran, in 2004, and the M.Sc. degree in Electronics Engineering from the Department of Electrical Engineering, RAZI University, Kermanshah, Iran, in 2010, (with honors), where, he is currently working toward the Ph.D. degree in Electronics Engineering. His research interests include RF and Microwave active and passive components.